Mobility spectrum computational analysis using a maximum entropy approach

S. Kiatgamolchai,* M. Myronov, O. A. Mironov,† V. G. Kantser,‡ E. H. C. Parker, and T. E. Whall
Department of Physics, University of Warwick, Coventry CV4 7AL, United Kingdom
(Received 22 January 2002; published 27 September 2002)

A method to calculate a smooth electrical conductivity versus mobility plot (''mobility spectrum'') from the classical magnetoconductivity tensor in heterogeneous structures with the help of a ''maximum entropy principle'' has been developed. In this approach the closeness of the fit and the entropy of the mobility spectrum are optimized. The spectrum is then the most probable one with the least influence of the personal bias of the investigator for any given set of experimental data and is maximally noncommittal with regard to the unmeasured data. The advantages of the maximum entropy mobility spectrum analysis as compared to the conventional mobility spectrum analysis are demonstrated using a synthetic dataset.

DOI: 10.1103/PhysRevE.66.036705 PACS number(s): 02.70.−c, 95.75.Pq

I. INTRODUCTION

The research and development of various types of modern electronic devices requires accurate modeling and analysis of transport phenomena. Using the semiclassical Boltzmann theory or the single-particle density matrix formalism [1], one can quantify the transport coefficients in the framework of the density functional theory [2]. For example, knowing the band structure and the phonon spectrum of a material, one can use the Bloch-Boltzmann equation and the linear response method to calculate the electron-phonon scattering probabilities and hence the experimentally measured electrical resistivity ρ and Hall coefficient R_H. An example of an application of such a complicated approach occurs in the case of *d* metals [3], but there are few others. Similar models that may be used to investigate the transport characteristics of semimetals and semiconductors include continuum-ensemble averaging and Monte Carlo simulations [4]. The latter, in particular, can explicitly take into account both the band structure and the various scattering processes. It permits direct computation of all quantities relevant to transport, such as carrier distribution function, density, velocity, etc., but unfortunately at the cost of long computation time and stochastic noise in the data.

All of the above approaches are very complex and meaningful comparisons of experimental results with theoretical predictions are difficult, especially for multicarrier systems (e.g., compound semiconductors, layered and device heterostructures with several different types of carriers). Since 1980s, new methods of examining experimental data on electrical transport have been developed. A ''mobility spectrum analysis (MSA)'' was proposed in the pioneering paper of Beck and Anderson [5], and developed [6,7] as a useful technique for analyzing galvanomagnetic phenomena. MSA transforms the electrical conductivity tensor versus magnetic field B into conductivity density $s(\mu)$ (defined below) versus mobility μ. This procedure replaces the commonly used parameters (carrier concentration, average mobility, and Hall coefficient) in the conventional transport approach. It is very important to note that MSA *does not require any a-priori assumptions* about the number of different types of carriers (carrier species).

The reduced-conductivity-tensor (RCT) scheme was devised [8] as an alternative to MSA for determination of the carrier densities and mobilities in multicarrier semiconductor systems. A matrix formalism of the magnetoresistance and Hall effect, based on the RCT, has also been further developed [9,10]. The MSA and RCT methods have been tested for many real systems such as Si, $Hg_xCd_{1-x}Te$, GaAs, and for various layered structures.

However, for both the MSA and RCT approaches it is almost impossible to ensure that the solution obtained does not contain unreliable negative values for the transport parameters. A major objective in our approach to MSA, presented in this paper, is to ensure that the solution obtained is always physically meaningful, i.e., everywhere positive. This is achieved using the maximum entropy principle (MEP) of information theory. The MEP method has been applied successfully in geophysical spectral analysis, beginning with the seminal work of Burg [11]. One can find examples of MEP applications in astronomy [12], neutron scattering [13], x-ray photoemission spectroscopy depth profiling [14], processing of nuclear magnetic-resonance spectra [15], electron-positron annihilation experiments [16], and in secondary-ion-mass spectrometry depth profile quantification by maximum entropy deconvolution [17].

The MEP method in data analysis is a variational approach. In the context of the analysis of transport phenomena, Sondheimer [18] was the first to discuss transport coefficients in metals, treating the Boltzmann integro-differential equation as a variational problem. This approach is based on the principle of maximum production of physical entropy or the entropy principle (EP) and is a minimization procedure, which in mathematical aspect is similar to that developed in our paper. Later work has established that the variational method of transport coefficients takes rigorous account of the band structure and of anisotropic scattering mechanisms in semimetals [19] and semiconductors [20].

*Present address: Department of Physics, Chulalongkom University, Bangkok 10330, Thailand.

†Author to whom correspondence should be addressed. Email address: O.A.Mironov@warwick.ac.uk

‡On leave from LISES Institute of Applied Physics ASM, Kishinev MD-2028, Moldova.

The variational approach is very useful for theoretical studies of transport phenomena in magnetic fields [19,20]. It has been used to describe the transport coefficients of bismuth materials [21,22] and narrow gap semiconductors such as lead telluride [20] with highly anisotropic effective masses and in a wide range of (nonquantum) magnetic fields. Recently, the variational method and the EP have been used to analyze the transport properties of semiconductor quantum wells [23]. We have outlined some peculiarities of the variational method for transport phenomena, because in the present maximum entropy approach we also aim to realize a suitable tool for the possible study of energy-dependent relaxation times and band structure features, as suggested by Beck and Anderson [5].

The major aim of this paper is to present mobility spectrum formalism based on the MEP and to demonstrate the advantages of maximum entropy mobility spectrum analysis (ME-MSA). The paper is organized as follows: in Sec. II a brief review of the various MSA methods is given. The basic ME-MSA approach is introduced in Sec. III, and it is shown how it might be used to obtain carrier densities and mobilities for different types of carriers on the basis of the MEP. The application of the ME-MSA to synthetic datasets is discussed in Sec. IV. The paper concludes in Sec. V with a discussion of the advantages of ME-MSA in comparison with earliest MSA approaches.

II. MOBILITY SPECTRUM APPROACH

MSA is a multicarrier characterization tool that employs the magnetic-field-dependent resistivity $\rho_{xx}(B)$ and Hall resistivity $\rho_{xy}(B)=BR_H(B)$. It is capable of treating different groups of carriers (carrier species) identified according to their different average mobilities, and hence different responses to the classical magnetic field. Using a set of experimental data points $(B,\rho_{xx}(B),\rho_{xy}(B))$, the magnetoconductivity[1] tensor components $\sigma_{xx}(B)$ and $\sigma_{xy}(B)$ can be obtained from the relations:

$$\sigma_{xx}(B)=\frac{\rho_{xx}(B)}{[\rho_{xx}(B)]^2+[B\rho_{xy}(B)]^2}, \tag{1a}$$

$$\sigma_{xy}(B)=\frac{BR_H(B)}{[\rho_{xx}(B)]^2+[B\rho_{xy}(B)]^2}. \tag{1b}$$

These tensor components are related to the mobility-dependent conductivity density $s(\mu)$ by the integral transforms:

$$\sigma_{xx}(B)=\int_{-\infty}^{\infty}\frac{s(\mu)}{1+(\mu B)^2}d\mu, \tag{2a}$$

$$\sigma_{xy}(B)=\int_{-\infty}^{\infty}\frac{s(\mu)\mu B}{1+(\mu B)^2}d\mu \tag{2b}$$

derived by Beck and Anderson [5]. In their pioneering paper they transformed the McClure integrals [24] over k space into integrals [Eqs. (2a) and (2b)] over the mobility μ and have introduced the electrical conductivity density function $s(\mu)$ called the carrier mobility spectrum. Similar density functions can be defined in a conventional transport approach: $s(k)$ in wave vector space and $s(E)$ in energy space. However, only the mobility spectrum $s(\mu)$ can be obtained immediately from the experimental magnetoconductivity data $\hat{\sigma}(B)$ using an inverse Laplace transformation and it contains all the information that can be extracted from $\hat{\sigma}(B)$. Therefore, MSA is very useful from the practical point of view and it has become a new approach for characterizing magnetotransport in conducting solids.

The reason that Beck and Anderson chose McClure's expression [24] as the starting theoretical concept is because it is valid at any arbitrary magnetic-field strength and the relaxation time is allowed to depend on the energy and crystal momentum in the magnetic-field direction, provided the relaxation time is constant on the cyclotron orbit. This should be compared with other Boltzmann transport approaches that are valid only in low or high classical magnetic fields [25]. A parabolic dependence of energy on crystal momentum is not assumed when deriving Eqs. (2a) and (2b) from McClure's expression. Beck and Anderson argue that if $s(\mu)$ can be solved accurately, rather than merely obtaining the envelope, it will provide all the information that can possibly be extracted from the magnetoconductivity, which can be summarized as follows. (1) the conductivities of different carrier species can be identified by distinct peaks in $s(\mu)$; (2) the broadening of each peak will indicate an energy dependence of the relaxation time; (3) if the constant-energy ''surface'' is anisotropic (i.e., nonspherical),[2] the $s(\mu)$ spectrum of a given group of carriers will contain several peaks that are the components of the mobility tensor; (4) constant-energy ''surfaces'' with both concave and convex sectors will result in both holelike and electronlike terms in Eq. 2(b).

This method has been applied to a number of different semiconductor materials, for example bulk-HgTe [26], thin film HgTe [27], bulk-$Hg_xCd_{1-x}Te$ [28], thin film $Hg_xCd_{1-x}Te$ [29], HgTe-CdTe superlattices [30], $Al_xGa_{1-x}As/GaAs$ heterostructures [31], Si–δ-doped GaAs [32] $In_xGa_{1-x}As/InP$ heterostructures [33], Si–δ-doped InSb [34], InP on a semi-insulating substrate [35], and SiGe/Si heterostructures [36].

For any measured set of data, the first mathematical procedure to obtain $s(\mu)$ as a solution to Eqs. (2a) and (2b) was developed by Beck and Anderson [5]. However, because the number of data points is finite, it is impossible to determine $s(\mu)$ uniquely by this method. In fact, the proposed procedures can only provide an envelope of all possible mobility spectrum solutions. This envelope can be regarded as yielding the maximum conductivity at each mobility that the measured material might have. Nevertheless, the $s(\mu)$ peaks in this envelope have been shown to provide good approximations to the mobility and carrier concentration of each carrier species.

[1] All conductivities, resistivities, and carrier densities referred to in this paper are equivalent 2D or ''sheet'' values.

[2] Contour in the case of a two-dimensional carrier gas.

Subsequent developments in the mobility spectrum approach have involved mathematical techniques that improved the accuracy of the obtained $s(\mu)$ values. Dziuba and Gorska [6,37] have transformed Eqs. (2a) and (2b) into their discrete forms

$$\sigma_{xx}(B_j)=\sum_{i=1}^{N}\frac{s_i}{1+\mu_i^2B_j^2}, \tag{3a}$$

$$\sigma_{xy}(B_j)=\sum_{i=1}^{N}\frac{s_i\mu_iB_j}{1+\mu_i^2B_j^2}, \tag{3b}$$

which are similar to those used in a nonlinear least-squares fit [38]. Thus, the partial conductivity s_i, and mobility μ_i, $(i=1,2,\ldots,N)$ in Eqs. (3a) and (3b) can be iteratively solved by using the Marquardt algorithm [39]. In the mobility spectrum calculation, N represents the number of mobilities which are arbitrarily defined to cover a wide range of likely mobilities of all carriers. It should be large enough so that a resultant set of partial conductivities s_i is virtually quasicontinuous, and is equivalent to the conductivity density $s(\mu)$. As a result, the term ''mobility spectrum'' usually refers to either a set of partial conductivities s_i and mobilities μ_i or a conductivity density $s(\mu)$. Taking all data points into account, Eqs. (3a) and (3b) constitute two systems of equations, which are linear in s_i. A set of partial conductivities s_i is deduced by a simple iterative technique [6]. The plot of s_i versus μ_i oscillates around zero partial conductivity with the biggest positive partial conductivity occurring at the mobility corresponding to the actual average mobility of the majority group of carriers in the material. The oscillation means that some of the partial conductivity is *negative*, which is *unphysical*. An additional ''smoothing procedure'' has been proposed to minimize this effect but it is found that the negative partial conductivity cannot be entirely suppressed while maintaining an acceptable fit to the data. In this iterative technique, a set of mobility points μ_i is arbitrarily chosen in the range $B_{\min}^{-1}$ to $B_{\max}^{-1}$, where $B_{\min}$ and $B_{\max}$ are the minimum and maximum measured magnetic fields. The number of mobility points is then limited by the number of measured magnetic-field points and the lowest mobility is set by the maximum magnetic field available.

An extended version of the iterative technique has been developed by Antoszewski *et al.* [40], which is known as quantitative mobility spectrum analysis (QMSA). In QMSA, the Gauss-Seidel successive over-relaxation iteration method is employed to give faster convergence and the partial conductivities are constrained to be non-negative at all iteration steps. The mobility range has been extended[3] to values of μ less than $B_{\max}^{-1}$ by extrapolation of the experimental data to higher fields than the maximum measured magnetic field [41]. A higher number of mobility points is also obtained by spline interpolation between the experimental data points. Even though these procedures seem to overcome problems inherent in the iterative technique, the use of interpolation and/or extrapolation of experimental data is questionable because there are several interpolation and extrapolation techniques available, and the modification of original data prior to calculation is subject to investigator bias and error.

An improved QMSA (*i*QMSA) [7] has removed the limitation in the number of mobility points by not confining these to the values $\mu_i=B_i^{-1}$. The range of mobilities and the number of mobility points are then independent of the range and the number of points of measured magnetic field, respectively. *i*QMSA differs from the iterative technique and QMSA, where it minimizes the least-squares deviation of both the conductivity tensor and its derivative with respect to the magnetic field. In addition, empirical procedures (two/three-point swapping and point elimination) for manipulating the mobility spectrum are introduced and shown to improve the fits while smoothing the spectrum and making it ''more physically reasonable.'' Despite these refinements, it must be said that empirical procedures are likely to be case specific and are dependent on the individual bias.

III. ME-MSA FORMALISM

In correspondence with earlier variants of the MSA method, the conductivity tensor components can be expressed as a fine grid of possible mobilities:

$$\sigma_{xx}(B_j)=\sum_{i}^{N}s(\mu_i)\cos^2\theta_{ij}=\frac{1}{2}\sigma_0+\frac{1}{2}\sum_{i=1}^{N}s(\mu_i)\cos 2\theta_{ij} \tag{4}$$

$$\sigma_{xy}(B_j)=\frac{1}{2}\sum_{i}^{N}s(\mu_i)\sin(2\theta_{ij}), \tag{5}$$

where θ_{ij} are the Hall angles of the carriers with mobility μ_i in magnetic field B_j and can be determined by the standard relation $\tan\theta_{ij}=\mu_iB_j$, $\sigma_0=\Sigma_{i=1}^{N}s(\mu_i)$ is the conductivity at zero magnetic field. In Eqs. (4) and (5) the function of partial conductivity $s(\mu_i)$ has the form $s(\mu_i)=s_p(\mu_i)=e\mu_ip(\mu_i)$ for the holes, and $s_n(\mu_i)=-e\mu_in(\mu_i)$ for the electrons. It defines the mobility spectrum of holes in the positive part of the μ-coordinate axis, while in the negative part of the μ axis it defines the mobility spectrum of electrons.

Within our formalism both the holes and the electrons have *non-negative* partial conductivities, but their mobilities are positive and negative, respectively. It is natural to use such sign definitions of the carrier mobilities, because in a given electrical field E the holes and electrons have a different directions of the drift velocity $v_d^j=\mu_iE$. Therefore, the tensor component of the magnetoconductivity $\sigma_{xx}(B_i)$ is written in Eq. (4) as an even function of θ_{ij}, while the Hall component $\sigma_{xy}(B_j)$ is written as an odd function of θ_{ij}, and the peculiarities of multicarrier longitudinal and transverse magnetoconductivity are correctly reflected.

The task of the MSA method is to find those spectra that provide the best fit to the experimental data $\sigma_{xx}^{\text{expt}}(B_j)=\sigma_{xx}^{j}(\text{expt.})$ and $\sigma_{xy}^{\text{expt}}(B_j)=\sigma_{xy}^{j}(\text{expt.})$ at all values of the available experimental magnetic fields.

[3]No details of how the mobility range is extended are given in the original paper.

All the previous attempts to generate an accurate mobility spectrum were based on minimizing the deviations between the experimental data on the magnetoconductivity tensor and the fit given by equations similar to Eqs. (4) and (5). Beck and Anderson [5], Dziuba and Gorska [6], and Antoszewski *et al.* [40] minimized the deviations at a given magnetic field B_j by simultaneously adjusting the electron and the hole partial conductivities, $s(\mu_i)$ at the mobilities $\mu_i = B_j^{-1}$. The optimization procedure was extended in *i*QMSA [7] to fit the magnetoconductivity tensor and its first derivative/slope with respect to *B*. The purpose of the iteration procedure was to establish what combinations of carrier type, mobility, and concentration led to the smallest deviations.

The deviation squared was chosen as the quantity to be minimized in all previous approaches to MSA. For example, in *i*QMSA, the optimization procedure is based on the following squared deviation:

$$\chi_j^2 = \frac{(\Delta_{xx}^j)^2 + (\Delta_{xy}^j)^2 + (\Delta_{xx}^{*j})^2 + (\Delta_{xy}^{*j})^2}{N\{[\sigma_{xx}^j(\text{expt.})]^2 + [\sigma_{xy}^j(\text{expt.})]^2 + [\sigma_{xx}^{*j}(\text{expt.})]^2 + [\sigma_{xy}^{*j}(\text{expt.})]^2\}}, \tag{6}$$

where

$$\Delta_{\alpha\beta}^j \equiv \sigma_{\alpha\beta}^j(\text{expt.}) - \sigma_{\alpha\beta}^j, \tag{7}$$

$$\Delta_{\alpha\beta}^{*j} = B_j \left[\frac{\partial \sigma_{\alpha\beta}^j(\text{expt.})}{\partial B} - \frac{\partial \sigma_{\alpha\beta}^j}{\partial B} \right]_{B=B_i} \tag{8}$$

are the deviations for the conductivity tensor components and their slopes, respectively, at given magnetic field B_j. Here N is the total number of the pseudodata points.

The ME-MSA approach developed in this paper is based on a fundamentally different procedure as it optimizes the fit to the magnetoconductivity tensor components on the basis of the MEP [15]. The main concept is to consider the mobility spectrum $s(\mu_i)$ in the form of a probability distribution of several events, which are supposed to be associated with the discrete values of the mobility parameter μ_i ($i = 1,2,\ldots,N$). The corresponding probabilities p_i are assumed to be the reduced values of the corresponding partial conductivity $s(\mu_i)$:

$$p_i = \frac{s(\mu_i)}{\sigma_0}. \tag{9}$$

The probabilities p_i are unknown. All we know are the expected values of the magnetoconductivity tensor components $\sigma_{\alpha\beta}(B_j)$ and that the probabilities p_i are required to be positive, and to satisfy the normalization condition $\Sigma_i^N p_i = 1$. From the information theory viewpoint, prior to the measurement there are no data and the most probable distribution is an equal distribution amongst all events. As we obtain the first few data points, they allow us to adjust the probability distribution in such a way that it produces a good fit to the measured data. However, at this early stage, there are not enough data points to produce a unique probability distribution because the number of data points is less than the number of events. Consequently, there are many feasible probability distributions that agree well with all the data points. Rationally, one would prefer to choose the probability distribution, which is maximally noncommittal with regard to unavailable (i.e., unmeasured) data. Examples of unavailable data are those between two adjacent measured data points on the magnetic-field axis and data at higher magnetic fields than are practically available. Jaynes [42] has shown that the most likely probability distribution amongst feasible distributions can be found by assigning ''an entropy'' to each probability distribution and choosing the one with the highest entropy. It has recently been shown [43] that the concept of entropy and its increase can be understood in general as an ''amount of uncertainty'' as it is understood in information theory, without reference to either statistical mechanics or heat engines.

Thus our ME-MSA approach is to combine minimization of the fit deviation from measured data with the principle of *entropy maximization*. Using the probabilities p_i defined above, the entropy H is written as

$$H(s) = -\sum_{i=1}^{N} p_i \ln p_i. \tag{10}$$

From this universal expression an equal distribution of probabilities follows in the case of zero magnetic fields. Equation (10) describes in a unique way the amount of uncertainty represented by a given probability distribution and it is the only one which satisfies the condition of consistency imposed by the composition law [42]. Mathematically, the maximum entropy distribution has an important property that no possibility is ignored and it assigns a positive weight to every situation. In the context of our ME-MSA approach, it is very important to note that the conditional maximum of Eq. (10) can be found from a stationary property involving Lagrange multipliers, which will be introduced below, and that the condition $p_i \geqslant 0$ is always satisfied.

We have pointed out that the optimization approach of previous MSA versions is based on the minimization of squared deviations such as those given in Eq. (6) and used in *i*QMSA. In the framework of ME-MSA, this is equivalent to defining the entropy as $H = -\Sigma_{i=1}^N p_i^2$. The properties of such defined quantity are similar to Eq. (10), and its use in other applications leads to equivalent results [42,44]. However, the conditional maximum of entropy $H = -\Sigma_{i=1}^N p_i^2$ is impossible to find on the basis of a stationary property involving

Lagrange multipliers, because the distribution probability, which makes this quantity stationary subject to prescribed averages, does not in general satisfy the condition $p_i \geqslant 0$ [42,44]. The negative values of p_i [or $s(\mu_i)$] could appear in previously proposed variants of MSA. Therefore, the requirement $p_i \geqslant 0$ must be imposed at all stages of computation and analysis.

One of the more important advantages of the ME-MSA approach in comparison with previous MSA is that it does not allow unphysical negative conductivities. With the help of maximum entropy principle, it is now evident how to develop the *mathematical model* of ME-MSA. The problem reduces to the maximization of the entropy as given by Eq. (10) subject to the constraints of Eqs. (4) and (5), which can be written as dimensionless averages

$$\overline{\sigma}_j^{xx} = \frac{\sigma_{xx}(B_j)}{\sigma_0} = \sum_{i=1}^{N} p_i \cos^2 \theta_{ij} = \frac{1}{2} + \frac{1}{2} \sum_{i=1}^{N} p_i \cos 2\theta_{ij}, \tag{11}$$

$$\overline{\sigma}_j^{xy} = \frac{\sigma_{xy}(B_j)}{\sigma_0} = \frac{1}{2} \sum_{i=1}^{N} p_i \sin 2\theta_{ij}. \tag{12}$$

Using the Lagrange multipliers λ_j^c and λ_j^s $(j=1,2,\ldots,M)$, where M is the number of magnetic-field points, we can form the partial function:

$$z(\lambda_1^c,\ldots,\lambda_M^c,\lambda_1^s,\ldots,\lambda_M^s) = \sum_{j=1}^{N} \exp\left[-\sum_{j=1}^{M} \lambda_j^c \cos^2 \theta_{ij} \right] \exp\left[-\frac{1}{2} \sum_{j=1}^{M} \lambda_j^s \sin 2\theta_{ij} \right]. \tag{13}$$

Then the maximum-entropy probability distribution (distribution of partial conductivities) is given by

$$p_i = \exp\left[-\lambda_0 - \sum_{j=1}^{M} \lambda_j^c \cos^2 \theta_{ij} - \frac{1}{2} \sum_{j=1}^{M} \lambda_j^s \sin 2\theta_{ij} \right]. \tag{14}$$

The values of constant Lagrange multipliers can be determined from

$$-\frac{\partial}{\partial \lambda_j^c} \ln z = \overline{\sigma}_j^{xx},$$

$$-\frac{\partial}{\partial \lambda_j^s} \ln z = \overline{\sigma}_j^{xy},$$

$$\ln z = \lambda_0. \tag{15}$$

In addition to their dependence on the mobility μ, the functions $\cos\theta_{ij}$ and $\sin\theta_{ij}$ contain parameters B_j. The present maximum entropy approach allows us to estimate the averages of the derivatives with respect to magnetic field:

$$\frac{1}{\sigma_0} \frac{\partial \sigma_{xx}}{\partial B_j} = -\frac{1}{\lambda_j^c} \frac{\partial}{\partial B_j} \ln z,$$

$$\frac{1}{\sigma_0} \frac{\partial \sigma_{xy}}{\partial B_j} = -\frac{1}{\lambda_j^s} \frac{\partial}{\partial B_j} \ln z, \tag{16}$$

and thus to improve the ME-MSA optimization in a similar fashion to *i*QMSA.

The ME-MSA general formalism developed involves two sets of Lagrange multipliers λ_j^c and λ_j^s. Substituting Eq. (14) into Eqs. (11) and (12), we obtain two sets of M nonlinear equations

$$\sum_{i=1}^{N} \left\{ (\cos^2 \theta_{ij} - \overline{\sigma}_j^{xx}) \exp\left[-\sum_{j=1}^{M} \left(\lambda_j^c \cos^2 \theta_{ij} + \frac{1}{2} \lambda_j^s \sin 2\theta_{ij} \right) \right] \right\} = 0, \tag{17}$$

$$\sum_{i=1}^{N} \left\{ \left(\frac{1}{2} \sin 2\theta_{ij} - \overline{\sigma}_j^{xy} \right) \exp\left[-\sum_{j=1}^{M} \left(\lambda_j^c \cos^2 \theta_{ij} + \frac{1}{2} \lambda_j^s \sin 2\theta_{ij} \right) \right] \right\} = 0. \tag{18}$$

The $2M$ equations allow [45] us to determine $2M$ Lagrange multipliers λ_j^c and λ_j^s. The ME-MSA can be simplified as follows. Noting that

$$\sin^2 \theta_{ij} + \cos^2 \theta_{ij} = 1,$$

$$\frac{1}{2} \sum_{i=1}^{N} p_i \sin 2\theta_{ij} = \sum_{i=1}^{N} p_i \cos\theta_{ij} (1 - \cos^2 \theta_{ij})^{1/2},$$

and using the approximate relations

$$\sum_{i=1}^{N} p_i f(\cos\theta_{ij}) \approx f\left(\sum_{i=1}^{N} p_i \cos\theta_{ij} \right), \tag{19}$$

the two sets of Lagrange multipliers can be reduced to one, because in this case $\lambda_j^c = \lambda_j^s/2 = \lambda_j$.

In the ME-MSA method developed here the tensor components $\sigma_{xx}(B)$ and $\sigma_{xy}(B)$ are expressed through *cosine* and *sine* trigonometrical functions in Eqs. (4) and (5) and Eqs. (11) and (12), and are calculated as average values of these functions. The functions in true are linked through

trigonometric identities [see notes between Eqs. (18) and (19)] and Lagrange's procedure should be carried out on the basis of these restrictions. As a result, the $2M$-dimensional problem [Eqs. (17) and (18)] has been reduced to an M-dimensional one Eq. (20), where M is the number of magnetic-field points. This reduced procedure allows us to combine $\sigma_{xx}(B)$ and $\sigma_{xy}(B)$ datasets as $\bar{\sigma}_j^{\mathrm{tot}}=\bar{\sigma}_j^{xx}+\bar{\sigma}_j^{xy}$ and to simplify the software for the case of one set of linear equations, instead of for two sets of linear equations, which is more difficult to solve. For our ME-MSA version and associated software the number of Lagrange multipliers can exceed the number M and even $2M$ and this aspect is one advantage of the ME-MSA method. Therefore, we compensate for the reduction in the number of Lagrangian multipliers used. One can trust the $2M$ to M reduction procedure when the values of $\rho_{xx}(B)$ and $\rho_{xy}(B)$ are comparable at strong enough magnetic fields $\mu_i B_j \approx 1$, but this is a general condition for all versions of MSA. Moreover in ME-MSA, we have the possibility to extend the number of magnetic-field points outside the range of minimal and maximal values of the measured experimental points. In the future, we intend to modify ME-MSA software for calculations with two sets of Lagrange multipliers, and we suggest that the results will be very close to those presented here.

In the results Eqs. (17) and (18) reduce to a following single set:

$$\sum_{i=1}^{N}\left\{(K_{ij}-\bar{\sigma}_j^{\mathrm{tot}})\exp\left(-\sum_{j=1}^{M}\lambda_j K_{ij}\right)\right\}=0, \tag{20}$$

where

$$K_{ij}=\cos^2\theta_{ij}+\frac{1}{2}\sin\theta_{ij}=\frac{1}{2}(1+\cos 2\theta_{ij}+\sin 2\theta_{ij}), \tag{21}$$

$$\bar{\sigma}_j^{\mathrm{tot}}=\bar{\sigma}_j^{xx}+\bar{\sigma}_j^{xy}.$$

The probability distribution becomes

$$p_i=\exp\left[-\lambda_0-\sum_{j=1}^{M}K_{ij}\lambda_j\right]. \tag{22}$$

The mobility spectrum is then achieved by the iteration of Eq. (22), using successive approximation [46] and the following equation:

$$\lambda_j^{(\mathrm{new})}=\lambda_j^{(\mathrm{old})}-\alpha\left(\bar{\sigma}_j^{\mathrm{tot}}-\sum_{i=1}^{N}K_{ij}p_i\right). \tag{23}$$

Here α is an adjustable parameter, which allows us to iterate Eqs. (22) and (23) until the set of probabilities p_i converges. The value of α can be chosen by a trial and error procedure and is usually set to be less than unity for the stability of the computation (the so-called ''under-relaxation'' iteration). In general, α can take any value but being less than unity has proved to be a good choice and we have typically used $\alpha=0.1-0.5$.

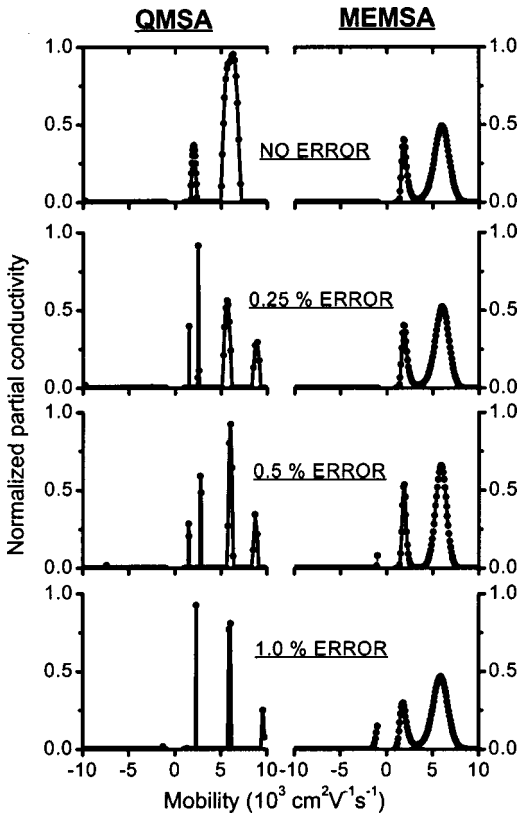

FIG. 1. Comparisons between QMSA and ME-MSA spectra of synthetic datasets for two carrier species ($n_1=1\times10^{11}$ cm^{-2}, $\mu_1=2000$ cm^2 V^{-1} s^{-1}; $n_2=1\times10^{11}$ cm^{-2}, $\mu_2=6000$ cm^2 V^{-1} s^{-1}), subject to various errors in ρ_{xx} and R_H. n_i is the sheet carrier density and μ_i is the mobility, with $i=1,2$.

IV. TESTING OF SYNTHETIC DATA

To demonstrate the ME-MSA technique, a synthetic dataset was generated and ME-MSA and QMSA analyses were performed. The synthetic dataset was calculated for two carriers with $n_1=1\times10^{11}$ cm^{-2}, $\mu_1=2000$ cm^2 V^{-1} s^{-1}; $n_2=1\times10^{11}$ cm^{-2}, $\mu_2=6000$ cm^2 V^{-1} s^{-1}, and with 30 magnetic-field points equally spaced from 0 to 10 T. The mobilities in the synthetic dataset are chosen to be high enough ($\mu_i B_{\max}>1$) so that the resultant mobility spectra can be obtained with high accuracy. The number of mobility points in the spectrum is 200, which are spaced equally in log scale for QMSA and linear scale for ME-MSA. The QMSA uses a cubic spline interpolation to obtain 200 data points, while ME-MSA uses only the available 30 data points. The mobility range is between 10^3 and 10^4 cm^2 V^{-1} s^{-1} for holes, and between -10^3 to -10^4 cm^2 V^{-1} s^{-1} for electrons, and the iteration continues until the spectrum does not change significantly, which is typically around 10^6 iterations for QMSA and 2×10^4 iterations for ME-MSA. The adjustable parameter α for all ME-MSA analyses, which gives smooth and stable convergence, is 0.2.

Figure 1 shows the normalized mobility spectrum obtained from both techniques for synthetic datasets with different errors in resistivity ρ_{xx} and Hall coefficient $R_H=(\rho_{xy}/B)$. For the ''no error'' case, both techniques yield

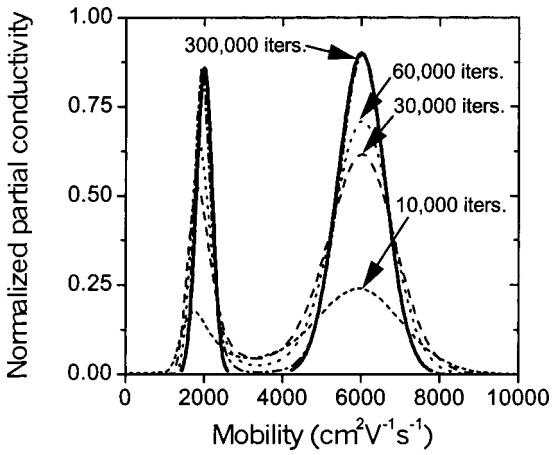

FIG. 2. ME-MSA spectrum for a synthetic dataset corresponding to two carrier species: ($n_1=1\times10^{11}$ cm^{-2}, $\mu_1=2000$ cm^2 V^{-1} s^{-1}; $n_2=1\times10^{11}$ cm^{-2}, $\mu_2=6000$ cm^2 V^{-1} s^{-1}). Each carrier species is assumed to have a Gaussian distribution of mobilities, which is represented by the thick solid line, with a fractional standard deviation of 0.1.

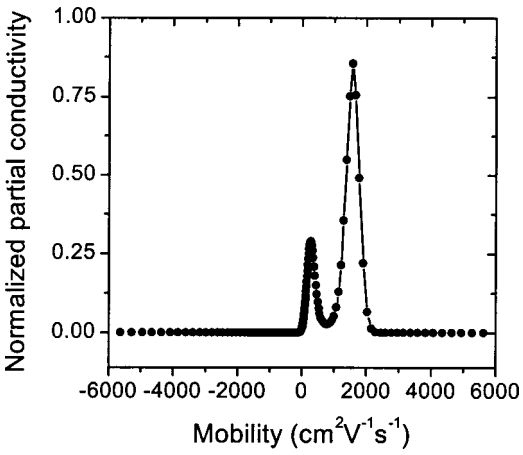

FIG. 3. ME-MSA spectrum of two carrier species ($n_1=1\times10^{11}$ cm^{-2}, $\mu_1=2000$ cm^2 V^{-1} s^{-1}; $n_2=1\times10^{11}$ cm^{-2}, $\mu_2=6000$ cm^2 V^{-1} s^{-1}), subject to 0.1% error in ρ_{xx} and R_H.

the same spectra consisting of two well-separated peaks, corresponding to two carrier species having mean mobilities of μ_1 and μ_2. As the errors increase, each peak in the QMSA spectrum splits into two sharp peaks while ME-MSA comfortably maintains its initial two peaks. Consequently, the number of carrier species obtained from ME-MSA will be much more accurate.

For higher values of error (0.5% and 1.0%), ME-MSA also starts to show an artifact around the electron mobility -1000 cm^2 V^{-1} s^{-1}. It should be noted that the initial peaks continue to dominate while the artifact is easily spotted as an incomplete peak.

Figure 2 demonstrates how the ME-MSA calculation evolves when the true mobility spectrum corresponds to Gaussian distributions. The ratio of the standard deviation to the mean mobility of the Gaussian distributions is set to be 0.1 and the true distributions are shown as solid lines. After 300 000 iterations, which take around 5 min on a computer running a 1-GHz Intel Pentium III processor, the ME-MSA closely resembles the true distribution.

The smoothness of ME-MSA is a very interesting feature that cannot be achieved by any other existing mobility spectrum technique. The shape of ME-MSA curves should provide information about the energy dependence of the relaxation time and the wave vector dependence of the constant energy ''surface,'' as first postulated by Beck and Anderson [5].

Another attractive feature of ME-MSA is the ability to recover the conductivity of low-mobility carriers below the limitation set by $B_{\max}^{-1}$, without any modifications to the main calculation and without the need for empirical procedures. To demonstrate this, a synthetic dataset was generated for two carriers having $n_1=1\times10^{13}$ cm^{-2}, $\mu_1=200$ cm^2 V^{-1} s^{-1}; $n_2=1\times10^{12}$ cm^{-2}, $\mu_2=1500$ cm^2 V^{-1} s^{-1}, with 0.1% error in ρ_{xx} and R_H, and 30 magnetic-field points equally spaced from 0 to 10 T. The ME-MSA was carried out for 500 000 iterations and the result is shown in Fig. 3. Two peaks at the mobilities μ_1 and μ_2 are clearly resolved. It should be noted that we choose mobilities that differ by an order of magnitude so that the low-mobility peak does not overlap the high-mobility peak.

To summarize, the ME-MSA technique can produce a mobility spectrum accurately, revealing the correct number of carrier species, and is less sensitive to experimental error. A good fit can be obtained within a reasonable calculation time and the low-mobility ($\mu_{\rm low}$) carrier contribution with $\mu_{\rm low}B_{\max}<1$ can be extracted successfully, provided the higher-mobility ($\mu_{\rm high}$) carrier has $\mu_{\rm high}B_{\max}\geqslant1.5$.

V. CONCLUSIONS

A powerful mathematical approach for investigations of multicarrier magnetotransport in heterogeneous materials and device structures has been proposed on the basis of the maximum entropy principle and the mobility spectrum analysis technique. The underlying idea of ME-MSA is to determine the probability distribution of the reduced partial conductivity using the concept of entropy maximization, subject to the constraints imposed by the conductivity-tensor components derived as probability weighted quantities and from experimental Hall and magnetoresistivity data. It results in a quantitative procedure for fitting multicarrier experimental data to theoretical forms and includes the following fundamental innovations.

(1) The standard unique formula for the entropy defines the probability as a reduced partial conductivity, unphysical negative conductivities are avoided, and the requirement of non-negative conductivities is not imposed during iteration.

(2) The conditional extremum of the entropy and other functionals can be found on the basis of a stationary property involving Lagrange multipliers.

(3) The electron and hole mobilities of the *same magnitude* can be resolved by virtue of their different signs. This is due to introducing the idea of positive mobility for the holes and negative one for the electrons, due to their opposite drift directions in a given electric field.

(4) The iteration and fitting procedures are improved by the use of exponential functions in the minimization processes, in contrast to the power functions used in conventional MSA approaches.

(5) The number of mobility points chosen is not limited to the number of magnetic-field points and can be higher leading to a reduction in errors.

(6) A knowledge of the partial conductivity at a given mobility μ_i does not require a measurement at field $B_i = \mu_i^{-1}$.

(7) The range of available mobilities can be extended to much lower and higher values than $\mu = B_{\max}^{-1}$ and $B_{\min}^{-1}$, respectively.

In order to demonstrate the advantages of the ME-MSA approach over the QMSA approach and other MSA variants, computations were carried out on a synthetic dataset, using both the ME-MSA and the QMSA iterative algorithms. While the QMSA spectra tend to collapse to a discrete set of δ functions, ME-MSA preserves linewidth information when runs are extended to a large number of iterations. Therefore, we expect that this technique will serve as a suitable tool for the study of energy-dependent relaxation times and band structures, as predicted by Beck and Anderson [5]. These advantages, in combination with the *a priori* exclusion of negative partial conductivities in accordance with the principle of maximum entropy and the sign separation of the mobility axis for electrons and holes, make ME-MSA a powerful approach for obtaining quantitative mobility and carrier density information. It has been demonstrated that ME-MSA gives a reduced level of errors compared to other MSA techniques and yields useful results when the errors in the magnetoresistivity tensor components are 0.25%, which is realistically attainable in most experiments. It is important to note that the ME-MSA algorithm is fully under computer control and does not require any supporting procedures on the part of the user.

ACKNOWLEDGMENTS

The authors would like to thank G. Rowlands, Z. Dziuba, A. Lusakowski, N. P. Barradas, and S. A. Ostanin for helpful discussions. S. Kiatgamolchai is grateful to the Institute for the Promotion of Teaching Science and Technology (IPST) of Thailand for financial support of his study in the United Kingdom (DPST). V.K. wishes to thank the Royal Society of the United Kingdom for financial support during his stay at the University of Warwick. This work was supported by the INTAS-01-0184 project.

[1] W. Kohn and J. Lattinger, Phys. Rev. **108**, 590 (1957).
[2] W. Kohn and L. J. Sham, Phys. Rev. **140**, A1133 (1965).
[3] T. P. Beaulac, P. B. Allen, and F. J. Pinski, Phys. Rev. A **26**, 1549 (1982).
[4] D. C. Look, *Electrical Characterization of GaAs Materials and Devices* (Wiley, New York, 1989).
[5] W. A. Beck and J. R. Anderson, J. Appl. Phys. **62**, 541 (1987).
[6] Z. Dziuba and M. Gorska, J. Phys. III **2**, 99 (1992).
[7] I. Vurgaftman, J. R. Meyer, C. A. Hoffman, D. Redfern, J. Antoszewski, L. Faraone, and J. R. Lindemuth, J. Appl. Phys. **84**, 4966 (1998).
[8] J. S. Kim, D. G. Seiler, and W. F. Tseng, J. Appl. Phys. **73**, 8324 (1993).
[9] J. S. Kim, J. Appl. Phys. **84**, 292 (1998).
[10] J. S. Kim, J. Appl. Phys. **86**, 3187 (1999).
[11] J. P. Burg, Geophysics **37**, 375 (1972).
[12] S. F. Gull and J. G. Daniel, Nature (London) **272**, 686 (1978).
[13] R. J. Papoular and R. Gillon, in *Neutron Scattering Data Analysis*, edited by M. W. Johnson, IOP Conf. Proc. No. 107 (Institute of Physics, Bristol, 1990), p. 101.
[14] G. C. Smith and A. K. Livesey, Surf. Interface Anal. **19**, 175 (1992).
[15] M. A. Delsuc and T. E. Malliavin, Anal. Chem. **70**, 2146 (1998).
[16] I. Wilkinson, R. J. Hughes, Zs. Major, S. B. Dugdale, M. A. Alam, E. Bruno, B. Ginatempo, and E. S. Giuliano, Phys. Rev. Lett. **87**, 216401 (2001).
[17] D. P. Chu and M. G. Dowsett, Phys. Rev. B **56**, 15 167 (1997).
[18] E. H. Sondheimer, Proc. R. Soc. London, Ser. A **203**, 75 (1950).
[19] D. V. Gitsu, I. M. Golban, and V. G. Kantser, Phys. Status Solidi B **112**, 473 (1982).
[20] P. M. Tomchuk, V. A. Shenderovskii, P. N. Gorley, and N. P. Gavaleshko, Phys. Status Solidi B **118**, 433 (1983).
[21] D. V. Gitsu, I. M. Golban, and V. G. Kantser, Phys. Status Solidi B **113**, 59 (1982).
[22] D. V. Gitsu, I. M. Golban, and V. G. Kantser, Phys. Status Solidi B **113**, 497 (1982).
[23] A. Casian, Z. Dashevsky, V. Kantser, H. Scherrer, I. Sur, and A. Sandu, Phys. Low-Dimens. Semicond. Struct. **5/6**, 49 (2000).
[24] J. W. McClure, Phys. Rev. **101**, 1642 (1956).
[25] A. C. Beer, Solid State Phys. **4**, 18 (1963).
[26] W. A. Beck, F. Crowne, J. R. Anderson, M. Gorska, and Z. Dziuba, J. Vac. Sci. Technol. A **6**, 2772 (1988).
[27] J. R. Meyer, C. A. Hoffman, F. J. Bartoli, J. M. Perez, J. E. Furneaux, R. J. Wagner, R. J. Koestner, and M. W. Goodwin, J. Vac. Sci. Technol. A **6**, 2775 (1988).
[28] J. R. Meyer, C. A. Hoffman, P. J. Bartoli, D. A. Arnold, S. Sivananthan, and J. P. Fauries, Semicond. Sci. Technol. **8**, 805 (1993).
[29] Y. Gui, B. Li, G. Zheng, Y. Chang, S. Wang, L. He, and J. Chu, J. Appl. Phys. **84**, 4327 (1998).
[30] S. Hwang, Y. Lansari, Z. Yang, Jr., J. W. Cook, and J. F. Schetzina, J. Vac. Sci. Technol. B **9**, 1799 (1991).
[31] C. Colvard, N. Nouri, D. Ackley, and H. Lee, J. Electrochem. Soc. **136**, 3463 (1989).
[32] I. A. Panaev, S. A. Studenikin, D. I. Lubyshev, and V. P. Migal, Semicond. Sci. Technol. **8**, 1822 (1993).
[33] S. P. Svensson, W. A. Beck, D. C. Martel, P. N. Uppal, and D. C. Cooke, J. Cryst. Growth **111**, 450 (1991).
[34] I. A. Panaev, S. A. Studenikin, V. A. Tkachenko, O. A. Tkachenko, J. P. Heremans, D. L. Partin, D. T. Morelli, and C.

M. Thrush, Semicond. Sci. Technol. **11**, 1857 (1996).
[35] J. Achard, C. Guillot, F. Barbarin, M. Dugay, and E. Goumet, Appl. Surf. Sci. **142**, 455 (1999).
[36] G. Höck, M. Glöck, T. Hackbarth, H. J. Herzog, and E. Kohn, Thin Solid Films **336**, 141 (1998).
[37] Z. Dziuba, Acta Phys. Pol. A **80**, 827 (1991).
[38] H. Koser, O. Völlinger, and H. Brugger, Inst. Phys. Conf. Ser. **136**, 789 (1993).
[39] D. W. Marquardt, J. Soc. Ind. Appl. Math. **11**, 431 (1963).
[40] J. Antoszewski, D. J. Seymour, L. Faraone, J. R. Meyer, and C. A. Hoffman, J. Electron. Mater. **24**, 1255 (1995).
[41] J. R. Meyer, C. A. Hoffman, J. Antoszewski, and L. Faraone, J. Appl. Phys. **81**, 709 (1997).
[42] E. T. Jaynes, Phys. Rev. **106**, 620 (1957).
[43] E. H. Lieb and J. Yngvason, Phys. Today **53**(4), 32 (2000).
[44] E. T. Jaynes, IEEE Trans. Syst. Sci. Cybern. **4**, 227 (1968).
[45] N. Agmon, Y. Alhassid, and R. D. Levine, J. Comput. Phys. **30**, 250 (1979).
[46] J. M. Hollis, J. E. Dorband, and F. Yusef-Zadeh, Astrophys. J. **386**, 293 (1992).